NOVEMBER 1976 PPPL-1308

LOWER HYBRID PARAMETRIC INSTABILITIES NONUNIFORM PUMP WAVES AND TOKAMAK APPLICATIONS

BY

R. L. BERGER, L. CHEN, P. K. KAW
AND
F. W. PERKINS

PLASMA PHYSICS LABORATORY

PRINCETON UNIVERSITY
PRINCETON, NEW JERSEY

This work was supported by U. S. Energy Research and Development Administration Contract E(11-1)-3073. Reproduction, translation, publication, use and disposal, in whole or in part, by or for the United States Government is permitted.

DISCLAIMER

NOTICE

Printed in the United States of America.

Available from
National Technical Information Service
U. S. Department of Commerce
5285 Port Royal Road
Springfield, Virginia 22151
Price: Printed Copy $ * ; Microfiche $3.00

*Pages	NTIS Selling Price
1-50	$ 4.00
51-150	5.45
151-325	7.60
326-500	10.60
501-1000	13.60

Lower Hybrid Parametric Instabilities - Nonuniform Pump Waves and Tokamak Applications

R. L. Berger, L. Chen, P. K. Kaw, and F. W. Perkins
Plasma Physics Laboratory, Princeton University
Princeton, N. J. 08540

November 1976

PPPL-1308

Lower Hybrid Parametric Instabilities - Nonuniform Pump Waves and Tokamak Applications

R.L. Berger, Liu Chen, P.K. Kaw, and F.W. Perkins

Plasma Physics Laboratory, Princeton University

Princeton, N.J. 08540

ABSTRACT

Electrostatic lower hybrid "pump" waves are often launched into tokamak plasmas by structures (e.g. waveguides) whose dimensions are considerably smaller than characteristic plasma sizes. Such waves propagate in well-defined resonance cones and give rise to parametric instabilities driven by electron $\underset{\sim}{E} \times \underset{\sim}{B}$ velocities. The finite size of the resonance cone region determines the threshold for both convective quasimode decay instabilities and absolute instabilities. The excitation of absolute instabilities depends on whether a travelling or standing wave pump model is used; travelling wave pumps require the daughter waves to have a definite frequency shift. Altogether, parametric instabilities driven by $\underset{\sim}{E} \times \underset{\sim}{B}$ velocities occur for threshold fields significantly below the threshold for filamentation instabilities driven by pondermotive forces. Applications to tokamak heating show that nonlinear effects set in when a certain power-per-wave-launching port is exceeded. For sufficiently high powers, these instabilities will occur in the low-density edge region of a tokamak. They are characterized by a daughter wave frequency 10% below the pump wave frequency - in agreement with experimental observations.

I. INTRODUCTION

One of the principal approaches to radio-frequency heating of tokamak devices is the use of lower hybrid radiation introduced by phased waveguide arrays.[1] By the term lower hybrid radiation, we mean waves which are principally electrostatic and which have a frequency at or above the local lower hybrid frequency. These waves obey the dispersion relation given in Eq. (7) below.

The power levels sufficient to heat tokamaks greatly exceed the uniform-medium parametric instability threshold suggesting the importance of nonlinear effects. Indeed, experimental results[2,3] have shown that parametric decay instabilities occur and that a correlation exists between the presence of parametric instabilities and ion heating. The observed thresholds, however, are well above those predicted by uniform medium theory.

Lower hybrid radiation heating of tokamaks therefore raises important questions in nonlinear wave-plasma interactions: will the nonlinear heating be so strong as to deposit the energy in only the surface layers? Can nonlinear heating be entirely avoided so that only linear absorption processes take place? Will nonlinear processes heat electrons or ions? How will tokamak geometries differ from the uniform medium calculations? And most importantly, how will all these processes scale as tokamak devices become larger and hotter?

This paper attempts to answer the question of how tokamak geometry affects the linear theory of lower hybrid parametric instabilities.[4-6] The key feature of tokamak heating schemes is that the monochromatic "pump" radiation is introduced through

phased-waveguide arrays whose dimensions are considerably smaller than the characteristic plasma sizes (see Fig. 1). The lower hybrid radiation emanating from these arrays propagates in well-defined resonance cones. Consequently, the most important spatial nonuniformities are those associated with the spatial variation of the pump intensity. As a specific example, consider a wave-launching grill that has a dimension $\lambda_o/2 \approx 15$ cm along the magnetic field. Then Eqs. (10) and (11) below show that the resonance cone has a radial extent of

$$\Delta r \sim \frac{\lambda_o}{2}\left(\frac{Zm}{M}\right)^{1/2}\left(\frac{\omega_o^2}{\omega_{LH}^2} - 1\right)^{1/2} \sim 1\text{cm} \quad ,$$

which is much smaller than the minor radius of typical tokamak devices.

The principal goal of this paper is to investigate the linear theory of lower hybrid parametric instabilities via a model consisting of a nonuniform pump wave propagating in a resonance cone in an otherwise uniform plasma. The effects of density gradients, magnetic shear, etc., will be discussed in the final section. We shall consider two instability modes: convective decay into lower hybrid waves via quasimodes and four-wave absolute instabilities. Decay into two lower hybrid modes does not play an important role in tokamak heating. Also, the most unstable modes will have frequency shifts much larger than the ion-cyclotron frequency so that a variety of cyclotron instabilities can be ignored. A second goal is to compare the threshold for exciting parametric instabilities driven by electron

$\underset{\sim}{E} \times \underset{\sim}{B}$ velocity with that of the filamentation instability recently proposed by Morales and Lee[7] as an explanation for the experimental observations of Gekelman and Stenzel.[8] The symmetry assumed in the Morales-Lee paper suppresses any nonlinear effects due to electron $\underset{\sim}{E} \times \underset{\sim}{B}$ velocities. In the theory of lower hybrid parametric instabilities by contrast, $\underset{\sim}{E} \times \underset{\sim}{B}$ velocities are by far the most dominant coupling term.

Porkolab[4] has presented a general discussion of lower hybrid waves in a nonuniform media. This paper employs the same general concepts, but includes group velocity propagation both transverse to and along the magnetic field for the purpose of determining which waves have the maximum growth. It is necessary to maximize the spatial amplification over all possible daughter wave frequencies and wave numbers to find which instabilities actually exist.

The travelling wave nature of the pump has important consequences for absolute instabilities. The review article by Nishikawa and Liu[9] showed that a travelling wave pump produces instabilities with a finite frequency shift from the pump. This means that one of the two high-frequency daughter waves is no longer resonant, so that the purely growing mode evolves into a convective quasimode. Nishikawa and Liu did not treat a spatially localized travelling wave pump.

Our model is presented in Sec. II. Section III discusses absolute four-wave instabilities, while Sec. IV addresses convective quasimode decay processes. The paper concludes with a discussion of tokamak applications.

II. MODEL AND EQUATIONS

Our starting point is a model of a uniform plasma with a straight magnetic field in the z-direction, and containing monochromatic lower hybrid pump radiation propagating in a resonance cone in the x-z plane. The plasma is composed of electrons at temperature T_e and ions of charge Z and mass M at a temperature T_i. The peak energy density of the pump radiation satisfies the inequality $E^2/8\pi nT_e << 1$ so that radiation pressure forces are negligible. As Eq. (75) below demonstrates, this restriction is consistent with the power levels required to heat tokamak research devices and reactors. While the pump wave propagates solely in the x-z plane, $\underset{\sim}{E} \times \underset{\sim}{B}$ coupling will be important only if the daughter waves have a component of their wave vector in the y-direction. We take this y-dependence to be sinusoidal - a simplification justified by the fact that the spatial inhomogenity of pump fields in tokamaks is much weaker in the y-direction than in the x-direction.

A cold plasma, electrostatic model will be employed to describe both the pump and daughter lower hybrid waves. According to this model, the electron and ion velocities are governed by the equations

$$\frac{d}{dt}\,\underset{\sim}{v}_i = -\frac{Ze}{M}\,\underset{\sim}{\nabla}\phi \quad , \qquad \frac{d}{dt}\,v_{||e} = \frac{e}{m}\,\nabla_{||}\phi \quad , \tag{1}$$

$$\underset{\sim}{v}_{\perp e} = \frac{-(\underset{\sim}{\nabla}\phi \times \underset{\sim}{z})c}{B} + \frac{c}{B\Omega_e}\,\frac{d}{dt}\,\underset{\sim}{\nabla}_\perp\phi \quad . \tag{2}$$

Next, we introduce what amounts to a two time scale linearization of (1) and (2). This is accomplished by letting

$$\frac{d}{dt} \to \frac{\partial}{\partial t} + (\gamma + \gamma_L) \equiv \frac{\partial}{\partial t} + \bar{\gamma} \quad , \tag{3}$$

where $\partial/\partial t$ operates only on the rapidly varying, purely oscillatory time dependence of $\underset{\sim}{v}_i$, ϕ, etc. The physical interpretation is that γ represents the growth rate of the instability while γ_L is the linear damping decrement given in Eq. (9). Because the damping decrement depends on wavenumber, our tacit assumption of a constant decrement is not rigorous, but introduces no serious errors.

The density continuity equations complete our fundamental set of equations:

$$\left(\frac{\partial}{\partial t} + \bar{\gamma}\right) n_{i,e} = -\underset{\sim}{\nabla} \cdot \left(n \underset{\sim}{v}_{i,e}\right) \quad . \tag{4}$$

Let us now specialize to the case of absolute instabilities which will require a full wave treatment; geometric optics will suffice for convective quasimodes. The nonlinear coupling between low-frequency density fluctuations and the daughter lower hybrid waves arises from the term on the right-hand side of (4) involving the pump wave $\underset{\sim}{E} \times \underset{\sim}{B}$ velocity of the electrons. Only terms first order in nonlinear coupling and $\bar{\gamma}$ will be retained.

Equations (1-4) can be combined so as to produce an equation governing lower hybrid daughter waves. This is accomplished by operating on (4) with operator (3) and utilizing (1), (2), Poisson's equation, the relationship $\partial^2/\partial t^2 = -\omega^2$ valid for any small amplitude wave, and the linearized operator inversion

$$\left(-\omega^2 + 2\gamma \frac{\partial}{\partial t}\right)^{-1} = -\frac{1}{\omega^2}\left(1 + \frac{2\gamma}{\omega^2}\frac{\partial}{\partial t}\right) . \tag{5}$$

The resulting equation is

$$\left(1 + \frac{\omega_{pe}^2}{\Omega_e^2} - \frac{\omega_{pi}^2}{\omega^2}\right) \underset{\sim}{\nabla}_\perp^2 \phi - \frac{\omega_{pe}^2}{\omega^2} \nabla_{||}^2 \phi \tag{6}$$

$$= \frac{2\bar{\gamma}}{\omega^2} \frac{\partial}{\partial t}\left[\frac{\omega_{pe}^2}{\omega^2} \nabla_{||}^2 \phi + \frac{\omega_{pi}^2}{\omega^2} \underset{\sim}{\nabla}_\perp^2 \phi\right] - \frac{\partial}{\partial t} \underset{\sim}{\nabla}\left(\frac{\omega_{peL}^2}{\Omega_e \omega^2}\right) \cdot \left(\underset{\sim}{\nabla} \phi_0 \times \underset{\sim}{z}\right) ,$$

where ϕ_0 is the potential of the pump wave and $\omega_{pe,L}^2$ denotes the fluctuations in plasma frequency associated with the low-frequency wave.

Looking forward to the next section, our treatment of quasimode decay processes will employ a geometrical optics model for daughter wave propagation. When the small terms on the right-hand side of (6) are ignored, the familiar geometrical optics dispersion relation is recovered

$$\omega^2 = \omega_{LH}^2 \left[\frac{k_{||}^2}{k_\perp^2} \left(\frac{M}{Zm} \right) + 1 \right] \quad , \tag{7}$$

$$\omega_{LH}^2 = \omega_{pi}^2 / (1 + \omega_{pe}^2 / \Omega_e^2) \quad , \tag{8}$$

and

$$\omega_{pi}^2 = \frac{4\pi Z n_e e^2}{M} \quad .$$

The damping decrement comes from straightforward kinetic theory

$$\gamma_L = \frac{\sqrt{\pi}}{2} \frac{\omega_{LH}^2}{\omega} \left(\frac{\omega^2 M}{k_\perp^2 Z T_i} \right) \left[Z \left(\frac{M}{2T_i} \right)^{1/2} \frac{\omega}{k_\perp} \exp(-M\omega^2 / 2k_\perp^2 T_i) \right. \tag{9}$$

$$\left. + \frac{T_i}{T_e} \left(\frac{m}{2T_e} \right)^{1/2} \frac{\omega}{k_{||}} \exp(-m\omega^2 / 2k_{||}^2 T_e) \right] + \frac{\nu_e}{2} \left(\frac{\omega_{pe}^2}{\Omega_e^2 + \omega_{pe}^2} + \frac{\omega^2 - \omega_{LH}^2}{\omega^2} \right)$$

where ν_e is the electron-ion collision frequency.

The next step is to rescale the z variable according to the relation

$$\bar{z} = z \left(\frac{Zm}{M} \right)^{1/2} \left(\frac{\omega_o^2}{\omega_{LH}^2} - 1 \right)^{1/2} \quad , \tag{10}$$

where ω_o is the angular frequency of the pump wave. The two daughter waves will have frequencies of $\omega \pm \omega_o$, with ω being the frequency of the low-frequency mode ($\omega_o >> \omega$). Equation (6)

becomes

$$\left(\nabla_{\perp}^2 - \frac{\partial^2}{\partial \bar{z}^2}\right)\phi = \mp \frac{2\omega_o \omega}{(\omega_o^2 - \omega_{LH}^2)} \frac{\partial^2 \phi}{\partial \bar{z}^2} - \frac{\omega_{LH}^2}{\Omega_i (\omega_o^2 - \omega_{LH}^2)} \frac{\partial}{\partial t} \frac{\nabla n_L}{n} \cdot (\nabla \phi_o \times z)$$

$$+ \frac{2\bar{\gamma}}{\omega_o^2} \frac{\partial}{\partial t} \left[\frac{\partial^2}{\partial \bar{z}^2} + \frac{\omega_{LH}^2}{\omega_o^2 - \omega_{LH}^2} \nabla_{\perp}^2\right] \phi \qquad (11)$$

where, in the nonlinear and damping terms, we can safely ignore the difference between the daughter and pump wave frequencies.

Figure 2 introduces the coordinate transformation which will greatly simplify the algebraic tasks ahead. In terms of the new variables.

$$\xi = \frac{x - \bar{z}}{\sqrt{2}} , \quad \eta = \frac{x + \bar{z}}{\sqrt{2}} , \quad y \equiv y , \qquad (12)$$

In addition, we note that the lowest order solution is obtained by setting the left-hand side equal to zero. Since the last term in (11) is small, we can replace ϕ to first approximation by its lowest order solution. Equation (11) becomes

$$\left(2 \frac{\partial^2}{\partial \xi \partial \eta} + \frac{\partial^2}{\partial y^2}\right)\phi = \mp \frac{w_o w}{(w_o^2 - 1)} \left(\frac{\partial}{\partial \eta} - \frac{\partial}{\partial \xi}\right)^2 \phi + \frac{\bar{\gamma}}{\omega_{LH}^2 (w_o^2 - 1)} \frac{\partial}{\partial t} \left(\frac{\partial}{\partial \eta} - \frac{\partial}{\partial \xi}\right)^2 \phi$$

$$+ \frac{1}{\sqrt{2}\, \Omega_i (w_o^2 - 1)} \frac{\partial}{\partial t} \frac{1}{n} \frac{\partial n_L}{\partial y} \left(\frac{\partial}{\partial \eta} + \frac{\partial}{\partial \xi}\right) \phi_o \qquad (13)$$

where we have defined the nondimensional frequencies $w_o = \omega_o/\omega_{LH}$, $w = \omega/\omega_{LH}$. As Fig. 2 makes clear, the pump wave depends only on ξ when dissipation processes are ignored.

What is the proper solution of (13) that corresponds to the pump wave propagating energy in the positive η-direction? Ignoring the last, nonlinear term on the right-hand side of (13), one finds that

$$\mathcal{E} = -\frac{\partial \phi}{\partial \xi} = \frac{1}{2\pi} \int_{-\infty}^{\infty} \mathcal{E}(k) \exp(-\lambda_k \eta) \exp[i(k\xi + \omega_k t)]dk \ , \qquad (14)$$

where

$$\lambda_k = \frac{\bar{\gamma} k}{2\omega_k} \left(\frac{w_o^2}{w_o^2 - 1} \right) << 1 \ ,$$

must be positive. This condition demands that k and ω_k [see (7)] have the same sign. The condition that $\mathcal{E}$ be real implies $\mathcal{E}(-k) = \mathcal{E}^*(k)$.

A simple expression for a propagating pump can be obtained when the attenuation λ_k is negligible One then finds

$$\mathcal{E}(\xi) = \left\{ \text{Real } \frac{1}{\pi} \int_{-\infty}^{\infty} \frac{E(\xi) i \exp(i\omega_o t)}{\xi - \xi' + i\varepsilon} d\xi' \right\} = E(\xi)\cos\omega_o t$$

$$- P \frac{1}{\pi} \int_{-\infty}^{\infty} d\xi' \frac{E(\xi')}{\xi - \xi'} \sin\omega_o t \equiv E_1 \cos\omega_o t + E_2 \sin\omega_o t \qquad (15)$$

with the relation

$$E_1 = E(\xi) = \frac{1}{2\pi} \int_{-\infty}^{\infty} \mathcal{E}(k) \exp(ik\xi) dk \tag{16}$$

in agreement with previous results.[10,11] The point that Eq. (15) makes is that a propagating pump wave must contain both $\cos\omega_o t$ and $\sin\omega_o t$ components. Equation (15) provides the relation between these components corresponding to energy propagation in the positive η-direction. Figure 3 portrays the function E_1 and E_2 associated with a split waveguide launcher:

$$E_1 = \begin{cases} 1 & 0 < \xi < \ell \\ -1 & -\ell < \xi < 0 \end{cases} \tag{17}$$

$$E_2 = \begin{cases} \frac{1}{\pi} \ell n \left(\frac{\xi^2 - \ell^2}{\xi^2}\right) & \xi^2 > \ell^2 \\ \frac{1}{\pi} \ell n \left(\frac{\ell^2 - \xi^2}{\xi^2}\right) & \xi^2 < \ell^2 \end{cases} \tag{18}$$

The E_2 function provides finite wave amplitudes outside of the geometrically defined resonance cone. The logarithmic divergences in E_2 stem from the discontinuities in E_1. At the plasma boundary, the E_2 function associated with the positive-z resonance cone precisely cancels the E_2 function associated with the negative-z resonance cone, while the corresponding E_1 functions add to give the electric field impressed by the waveguide launcher.

Our interest in pump propagation is to provide a correct description of the environment in which instabilities occur. Indeed, the frequency shifts for absolute instabilities are different for travelling-wave and standing-wave pumps. More extensive discussions of pump propagation can be found in papers devoted to the subject.[10,11]

The zero-order description for the daughter waves is obtained by neglecting the right-hand side of (13) with the result

$$\tilde{\phi} = \frac{1}{2}\left\{\phi_1(\xi)\exp\left[i\left(q\eta - \frac{k^2}{2q}\xi + ky - (\omega_o + \omega)t\right)\right]\right. \tag{19}$$

$$\left. + \phi_2(\xi)\exp\left[i\left(q\eta - \frac{k^2}{2q}\xi + ky + (\omega_o - \omega)t\right)\right] + c.c.\right\} .$$

The slow ξ-dependence of ϕ_1 and ϕ_2 will be determined from the nonlinear coupling equations.

Let us now turn our attention to the low-frequency equations. We shall assume that electrons achieve a hydrostatic balance along the magnetic field, but we will retain kinetic effects for the ions because the frequency ω of the low-frequency mode will turn out to be non-zero and, in fact, much larger than the ion-cyclotron frequency permitting us to neglect the magnetic field in the ion dynamics.

The hydrostatic balance equation for the equations is

$$nm\left\langle \underset{\sim}{v}_\perp \cdot \nabla_\perp v_{||} \right\rangle = \frac{nce}{B\omega_o^2} \left\langle (\nabla_\perp \phi \times \underset{\sim}{z}) \cdot \nabla_\perp \nabla_{||} \frac{\partial \phi}{\partial t} \right\rangle \tag{20}$$

$$= -T_e \nabla_{||} n_L + n_e \nabla_{||} \phi_L$$

and the $\langle\ \rangle$ brackets denote a time average

$$\langle\ \rangle \equiv \frac{1}{T} \int_o^T dt$$

with the time T selected to be long compared to the high-frequency daughter wave periods but short compared to the period of the low-frequency fluctuations. As a result, boundary terms can be neglected in integrations by parts and one obtains

$$\frac{nce}{2B\omega_o^2} \nabla_{||} \left\langle (\nabla_\perp \phi \times \underset{\sim}{z}) \cdot \nabla_\perp \frac{\partial \phi}{\partial t} \right\rangle = -T_e \nabla_{||} n_L + ne \nabla_{||} \phi_L \ . \tag{21}$$

Equation (21) is readily integrated to yield

$$n_L - n \exp\left[\frac{e\phi_L}{T_e} - \frac{ce}{2BT_e\omega_o^2} \left\langle (\nabla_\perp \phi \times \underset{\sim}{z}) \cdot \underset{\sim}{\nabla}_\perp \frac{\partial \phi}{\partial t} \right\rangle\right] \ , \tag{22}$$

where the potential ϕ includes both pump ϕ_o and daughter wave $\tilde{\phi}$ contributions, $\phi = \tilde{\phi} + \phi_o$. A further simplification of (22) results because ϕ_o depends only on ξ and not on y. Algebraic manipulations lead to the linearized expression

$$n_L = n\left(\frac{e\phi_L}{T_e} - \frac{e}{\omega_o T_e} \left\langle \frac{\partial \tilde{\phi}}{\partial y} U_o(\xi,t) \right\rangle\right) \quad , \tag{23}$$

where

$$U_o(\zeta,t) - \frac{1}{2}\left[U_o(\xi)\exp(i\omega_o t) + U_o^*(\xi)\exp(-i\omega_o t)\right] = \frac{\cap}{B\omega_o}\frac{\partial}{\partial t}\frac{\partial \phi_\cap}{\partial x} \tag{24}$$

Substituting (19) into (23), one finds that

$$\frac{n_L}{n} = \frac{e\phi_L}{T_e} - \frac{1}{4}\left\{\frac{iek}{\omega_o T_e}(\phi_1 U_o + \phi_2 U_o^*)\exp\left[i\left(q\eta - \frac{k^2}{2q}\xi + k_y - \omega t\right)\right] + c.c.\right\} . \tag{25}$$

The low-frequency ion dynamics is taken to be governed by the nonmagnetic Vlasov equation

$$\frac{\partial \tilde{f}}{\partial t} + \underset{\sim}{v}\cdot\tilde{\nabla}\tilde{f} - \frac{Ze}{M}\nabla\phi_L\cdot\frac{\partial f_o}{\partial \underset{\sim}{v}} = 0 \quad , \tag{26}$$

yielding an ion density fluctuation

$$\tilde{n}_i = -\frac{Zn_{oi}e\phi_L}{T_i} W_i \tag{27}$$

where

$$p = q + (k^2/2q)$$

is the magnitude of the daughter wave vector and $W_i = W(\omega/p\bar{v}_i)$. Here $W(s) = 1 + sZ(s)$ where $Z(s)$ is the plasma dispersion function. Combining (23-27) with the quasineutrality condition, one obtains the low-frequency density perturbation

$$\frac{n_L}{n} = \left\{ \frac{ike}{4\omega_o T_e} \quad (\phi_1 U_o + \phi_2 U_o^*) \; \frac{W_i}{[(T_i/ZT_e) + W_i]} \exp[i(qn - \frac{k^2}{2q}\,\xi + ky - \omega t)] + c.c. \right\} . \tag{28}$$

Our derivation of the equations governing lower hybrid parametric instabilities in a bounded pump is now complete. Equations (13), (19), and (28) form a coupled set of equations which are linear in the amplitude of the daughter waves and quadratic in the pump amplitude.

III. ABSOLUTE INSTABILITIES

The question posed in this section is: Can an absolute four-wave instability be generated by a pump wave spatially well defined by the resonance cone and propagating energy in the η-direction? Since our model will only generate daughter waves when the daughters have a finite y-component of propagation, the group velocity of the daughter waves will not be parallel to that of pump. Consequently, the daughter waves will propagate out of the resonance cone region and we must look for solutions with outward energy propagation.

The equations governing absolute instabilities come from the combination of (13), (19), and (28) which generates coupled equations for the two daughter lower hybrid waves.

$$2iq\,\frac{\partial \phi_1}{\partial \xi} = \frac{w_o(\omega + i\bar{\gamma})}{(w_o^2 - 1)\omega_{LH}}\left(q + \frac{k^2}{2q}\right)^2 \phi_1 \qquad (29)$$

$$- \frac{Mk^2\, W_i}{4ZT_e[W_i + (T_i/ZT_e)]}\,\frac{(\phi_1|U_o|^2 + \phi_2 U_o^{*2})}{(w_o^2 - 1)}$$

and

$$2iq\,\frac{\partial \phi_2}{\partial \xi} = -\frac{w_o(\omega + i\bar{\gamma})}{(w_o^2 - 1)\omega_{LH}}\left(q + \frac{k^2}{2q}\right)^2 \phi_2 \qquad (30)$$

$$- \frac{Mk^2\, W_i}{4ZT_e[W_i + (T_i/ZT_e)]}\,\frac{(\phi_1 U_o^2 + \phi_2|U_o|^2)}{(w_o^2 - 1)}$$

Still further algebraic manipulations utilizing the substitutions

$$\phi_1 = \psi_1(\zeta) \exp\left[\left(i\int_o^\zeta \frac{Mk^2 W_i |U_o|^2 \ell \, d\zeta}{8ZqT_e[W_i + (T_i/ZT_e)(w_o^2 - 1)]}\right)\right] \tag{31}$$

$$\phi_2 = -i\psi_2(\zeta) \exp\left[\left(i\int_o^\zeta \frac{Mk^2 W_i |U_o|^2 \ell \, d\zeta}{8ZqT_e[W_i + (T_i/ZT_e)(w_o^2 - 1)]}\right)\right] \tag{32}$$

$$\xi = \zeta\ell$$

reduce these equations to

$$\begin{aligned} \frac{\partial\psi_1}{\partial\zeta} &= \Lambda_1 \psi_1 + \Lambda_2 U^2 \psi_2 \\ \frac{\partial\psi_2}{\partial\zeta} &= -\Lambda_1 \psi_1 - \Lambda_2 U^{*2} \psi_1 \end{aligned} \tag{33}$$

with the definitions

$$\Lambda_1 = \frac{w_o(\bar{\gamma} - i\omega)p\ell}{2(w_o^2 - 1)\omega_{LH}}\left(\frac{2q^2 + k^2}{2q^2}\right) \tag{34}$$

$$\Lambda_2 = \frac{Mc^2 E_o^2 p\ell}{4B^2 ZT_e(w_o^2 - 1)} \quad \frac{W_i}{[W_i + (T_i/ZT_e)]} \quad \frac{k^2}{2q^2 + k^2} \tag{35}$$

$$U^2 = -(E_1 + iE_2)^2 \tag{36}$$

$$-\frac{\partial\phi_o}{\partial\zeta} = \frac{E_o}{2}\left[(E_1 - iE_2)\exp(i\omega_o t) + c.c.\right] \tag{37}$$

and E_1, E_2 are given in (17) - (18). The boundary conditions on (33) are that ψ_1, ψ_2 vanish as $|\zeta| \to \infty$.

What expression (35) says is that the threshold field required for absolute instabilities will decrease as the product $p\ell$ is increased. On the other hand, the wavenumber p cannot be indefinitely increased without incurring heavy electron-Landau damping. Therefore, in the region $\omega_o > \omega_{LH}(1 + T_i/T_e)^{1/2}$ where electron-Landau damping dominantes over ion-Landau damping, one is motivated to write p in terms of V_e

$$V_e = (\omega/k_{||})(m/T_e)^{1/2} \tag{38}$$

using the W.K.B. dispersion relation (7). This yields

$$p\ell = (\pi/V_e)(mc^2/T_e)^{1/2}(2L/\lambda_o) \tag{39}$$

λ_o denoting the vacuum wavelength associated with the pump frequency ω_o . Hence in the electron-Landau damping region, we find

$$Re(\Lambda_1) = \Lambda_{1R} = \frac{1}{2}\left(\frac{\pi}{2}\right)^{3/2}\left(\frac{mc^2}{T_e}\right)^{1/2}\left(\frac{2L}{\lambda_o}\right) V_e^2 \exp(-V_e^2/2)\left(\frac{2q^2 + k^2}{2q^2}\right) \tag{40}$$

$$Im(\Lambda_1) = \Lambda_{1I} = -\frac{\chi_i}{\sqrt{2}} \frac{w_o^2}{(w_o^2-1)^{3/2}} \frac{\pi}{V_e^2}\left(\frac{T_i}{ZT_e}\right)^{1/2}\left(\frac{mc^2}{T_e}\right)^{1/2}\left(\frac{2L}{\lambda_o}\right)\left(\frac{2q^2+k^2}{2q^2}\right) \tag{41}$$

$$\Lambda_2 = \frac{Mc^2E_o^2\,\pi}{4B^2ZT_e(w_o^2-1)V_e}\left(\frac{mc^2}{T_e}\right)^{1/2}\left(\frac{2L}{\lambda_o}\right)\left(\frac{W_i}{W_i + (T_i/ZT_e)}\right)\left(\frac{k^2}{2q^2 + k^2}\right) \tag{42}$$

with $\chi_i = \omega/p\bar{v}_i$ denoting the argument of the W_i function. For most practical circumstances, the length L of the phased waveguide array will be approximately $L = \lambda_o/2$ (see Fig. 1).

Formulas (40)-(42) permit us to reach some helpful conclusions. First, a value $V_e \approx 4$ is sufficiently large so that damping can be ignored. Conversely, when V_e takes on values $V_e < 4$, the plasma wave damping becomes severe and instabilities will not arise. Thus, with good accuracy, one can use $V_e = 4$ to compute the threshold fields via (42). Our second conclusion is that for moderate values of $\chi_i \lesssim 1$, the phase shift $\mathrm{Im}\Lambda_1$ can achieve significant values ($\mathrm{Im}\Lambda_1 \sim \pi$), especially when $2q^2 < k^2$. This corresponds to daughter wave propagation close to propagation direction for the pump. Consequently, Λ_2 will be almost real. Third, because $mc^2/T_e >> 1$, Λ_2 can achieve significant values for $c^2E_o^2M/B^2ZT_e \lesssim 1$ vindicating our weak coupling theory. The factors involving k^2, q^2 pertain to the orientation of the daughter wave vector in the plane perpendicular to the magnetic field. From the definition

$$\sin = (k_y/k_\perp) = (2\sqrt{2}\,kq) / (2q^2 + k^2) \quad , \tag{43}$$

one can show that

$$\frac{1-\cos\phi}{2} = \frac{2q^2}{k^2+2q^2} \; ; \; \frac{1+\cos\phi}{2} = \frac{k^2}{k^2+2q^2} \quad . \tag{44}$$

Clearly for only moderately small values of ϕ, one can make the phase shift Λ_{1I}, large, while hardly affecting the threshold field via Λ_2.

The upshot of this discussion is that one is led to consider a simplified version of (33), in which spatial damping is ignored ($\Lambda_{1R} = 0$):

$$\frac{\partial}{\partial \zeta} a = \Lambda_2 U^2 \exp(-2i\Lambda_{1I}\zeta) b$$

$$\frac{\partial b}{\partial \zeta} = - \Lambda_2 U^{*2} \exp(+2i\Lambda_{1I}\zeta) a \qquad (45)$$

with the boundary conditions,

$$\zeta \to \begin{cases} +\infty \ , \ a \to 0 \ , & b \ \text{const.} \qquad (46a) \\ -\infty \ , \ a \to \text{const.} \ , & b \ 0 \qquad (46b) \end{cases}$$

and the definitions

$$\psi_1 = a \exp(i\Lambda_{1I}\zeta) \ , \quad \psi_2 = b \exp(-i\Lambda_{1I}\zeta) \ . \qquad (47)$$

While the exact relationship between the eigenvalues Λ_1 and Λ_2 depends on the computational solutions reported below, it is quite instructive to solve the model problem

$$U^2 = \begin{cases} \exp(-2\pi i\zeta) & |\zeta| < 1 \\ 0 & |\zeta| > 1 \end{cases} \qquad (48)$$

which simulates a traveling wave pump by its monotonic progression in phase. The solution which obeys boundary condition (46a) is

$$a = \exp[-i(\Lambda_{1I} + \pi)\zeta] \sin\left\{(\zeta - 1)[\Lambda_2^2 + (\Lambda_{1I} + \pi)^2]^{1/2}\right\}$$

while boundary condition (46b) generates the eigenvalue equation

$$\tan\left\{2[\Lambda_2^2 + (\Lambda_{1I} + \pi)^2]^{1/2}\right\} = i[\Lambda_2^2 + (\Lambda_1 + \pi)^2]^{1/2} \; / \; (\Lambda_{1I} + \pi). \tag{50}$$

A solution is $\Lambda_{1I} = -\pi$, $\Lambda_2 = \pi/4$.

Neighboring solutions can be found by a perturbation approach. Defining

$$\Lambda_1 = i\pi + \delta\Lambda_1 \; , \; \Lambda_2 = \pi/4 + \delta\Lambda \; ,$$

obtains the relationship

$$\delta\Lambda_1 = \frac{\pi}{2}\,\delta\Lambda_2 \; . \tag{51}$$

The physical consequences of (51) is that small complex corrections to Λ_2 [(c.c.(35)] will not suppress absolute instabilities. The argument proceeds as follows: The real parts of $\delta\Lambda_1$ can be made zero (the threshold condition) by appropriate adjustment of E_o^2 [c.f.(35)] while any imaginary contributions to Λ_2 due to the finite argument of W_i can be balanced by the appropriate frequency shift in (34).

Figure 4 shows the results of computational solutions using the correct form for U_o, i.e.(17), (18), and (36). The role of ion dynamics is represented by the phase angle θ defined according to

$$\Lambda_2 = |\Lambda_2| \exp(i\theta). \tag{52}$$

The computational results bring out a key point. Over a good range of phase angles, $-1 < \theta < 1$, there are only small variations in the magnitude of Λ_2 . Consequently, the threshold condition is well represented by using $W_i = 1$ in (35).

Absolute instabilities characteristically have small frequency shifts. One can recast (41) to read

$$\frac{\omega}{\omega_o} = -\sqrt{2}\left(\frac{\Lambda_{1I}}{\pi}\right)\frac{w_o^2-1}{w_o^2}\,V_e\left(\frac{T_e}{mc^2}\right)^{1/2}\left(\frac{\lambda_o}{2L}\right)\frac{2q^2}{2q^2+k^2} \quad . \tag{53}$$

Numerically, Eq. (54) yeilds $\omega/\omega_o \sim (0.5\text{-}1)\cdot 10^{-1}$ for typical tokamak parameters, justifying our assumption that $\omega_o >> \omega >> \Omega_i$.

One can now check a posteriori that radiation pressure effects are small by recasting (42) into the form

$$\frac{E_o^2}{8\pi n T_e} \approx \frac{V_e}{2}\left(\frac{v_A^2}{c^2}\right)\left(\frac{T_e}{mc^2}\right)^{1/2}\left(\frac{\lambda_o}{2L}\right)\left(w_o^2-1\right) << 1$$

where $\Lambda_2 \approx \pi/4$ was used. Except at very low densities, parametric instabilities dominate over the self-focusing instabilities of Morales and Lee.[7]

IV. CONVECTIVE QUASIMODE INSTABILITIES

Convective decay instabilities can occur in the lower hybrid frequency regime via nonlinear damping on the electrons or ions. The uniform medium growth rates have been discussed exhaustively by Porkolab.[5] The goal of this section is to compute the spatial amplification, and maximize it over all possible wavevectors and frequencies of the daughter waves. The principal limitation of convective amplification is propagation of daughter wave energy away from the localized pump. This process always occurs, because as we shall show below, the group velocity of the daughter wave can never be precisely parallel to the pump. In our model, we shall assume that the pump wavelength greatly exceeds the wavelength of the daughter waves. This is justified by two arguments: First, we shall show that the shortest wavelength daughter waves undergo the largest amplification, hence any difference wavenumber $|\underset{\sim}{k}_1-\underset{\sim}{k}_o|$ is well approximated by the daughter wavenumber: $|\underset{\sim}{k}_1-\underset{\sim}{k}_o| \simeq |k_y|$. (This stems from the fact that the shortest wavelengths have the lowest group velocity.) Secondly, in contrast to the purely growing mode, feedback of energy plays no role in an amplification process so that gradual phase variations in the pump are unimportant.

Figure 5 sketches the geometry appropriate to the quasimode decay process. The standard theory for amplification gives

$$A = \int_{L_\xi} \frac{\gamma(\underset{\sim}{k}_1, \omega_0, \omega_1)}{V_{g\xi}(\omega_1, \underset{\sim}{k}_1)} \, d\xi \tag{54}$$

where γ is the uniform medium growth rate and $\underset{\sim}{k}_1$, ω_1 denote the wavevector and frequency of the daughter wave.

The group velocity of lower hybrid waves can be calculated in a straightforward manner from dispersion relation (7). The results are

$$V_{gz} = \frac{\omega^2 - \omega_{LH}^2}{k_{||}\omega} \quad ; \quad \underset{\sim}{V}_{g\perp} = -\frac{\omega^2 - \omega_{LH}}{\omega} \frac{\underset{\sim}{k}_\perp}{k_\perp^2} \quad . \tag{55}$$

Using (55), we can find directly that

$$V_{y\xi} = \frac{\underset{\sim}{V}_{g1} \cdot (\underset{\sim}{V}_{go} \times \hat{\underset{\sim}{y}})}{\sqrt{2}\ |\underset{\sim}{V}_{go}|} - \frac{\omega_1^2 - \omega_{LH}^2}{\sqrt{2}\omega_1 k_{\perp 1}} \left[\left(\frac{\omega_o^2 - \omega_{LH}^2}{\omega_1^2 - \omega_{LH}^2} \right)^{1/2} - \cos\phi \right] \tag{56}$$

where $\cos\phi = k_{x1}/k_{\perp 1}$ describes the orientation of the daughter wave number in the $\underset{\sim}{k}_\perp$ - plane. Porkolab's paper[5] presents a general formulation for the growth rate of lower hybrid parametric instabilities. Casting his Eq. (15) into our notation and ignoring the anti-Stokes term, one obtains

$$\varepsilon(\omega + \omega_o) = -i\bar{\gamma} \left(\frac{\partial \varepsilon}{\partial \omega_1} \right) = -\frac{c^2 E_o^2}{4B^2 \omega_o^2} k_y^2 \mathrm{Im} \left[\frac{\chi_i(\omega)\ [1 + \chi_e(\omega)]}{\varepsilon(\omega)} \right]$$

where $\omega = \omega_1 - \omega_o$, and we have assumed that the dispersion relation

$$\varepsilon(k, \omega_1) = 1 + \frac{\omega_{pe}^2}{\Omega_e^2} - \frac{\omega_{pe}^2 k_{||}^2}{\omega_1^2 k^2} - \frac{\omega_{pi}^2}{\omega_1^2} \frac{k_\perp^2}{k^2} = 0$$

is satisfied for the daughter lower hybrid wave. One then obtains

$$\bar{\gamma} = \gamma + \gamma_L = - \frac{c^2 E_o^2 M \omega_{LH}^2 \omega_1}{8B^2 Z T_e \omega_o^2} \sin^2\phi \qquad (57)$$

$$\text{Im} \left(\frac{(k^2 D_e^2 + W_e) W_i Z T_e / T_i}{k^2 D_e^2 + W_e + Z T_e W_i / T_i} \right)$$

where W is related to the plasma dispersion function Z via $W=1+zZ$. The subscripts specify the arguments of W:

$$W_i = W\left[\frac{\omega_1 - \omega_o}{k_\perp} \left(\frac{M}{2T_i}\right)^{1/2}\right] ; \; W_e = W\left[\frac{\omega_1 - \omega_o}{k_{||}} \left(\frac{m}{2T_e}\right)^{1/2}\right] . \qquad (58)$$

In the development below, we shall ignore the linear damping, γ_L except to note that it becomes very strong when the phase velocities become comparable to the thermal velocities, effectively preventing instabilities for low phase velocities.

Combining (54) - (58), one obtains

$$A = -\left(\frac{\sqrt{2}}{8} \int_{L_\xi} \frac{c^2 E_o^2(\xi) M}{B^2 Z T_e} d\xi \right) \frac{k_\perp w_1^2}{w_o^2 (w_1^2 - 1)} \qquad (59)$$

$$\left(\frac{\sin^2\phi}{(w_o^2-1)/(w_1^2-1)^{1/2} - \cos\phi} \right) \quad \text{Im} \left(\frac{(k^2 D_e^2 + W_e) T_e Z W_i / T_i}{k^2 D_e^2 + W_e + Z T_e W_i / T_i} \right)$$

Equation (59) shows that the dependence of the amplification on the daughter wavevector orientation ϕ and magnitude $k_{\perp 1}$ is separable. Hence one can maximize (59) over ϕ to obtain:

$$\max A = -\left(\frac{1}{2\sqrt{2}} \int_{L_\xi} \frac{c^2 E_o^2(\xi)}{B^2 T_e Z}\, d\xi\right) \frac{k_{\perp 1}[(w_o^2 - 1)^{1/2} - (w_o^2 - w_1^2)^{1/2}]w_1^2}{(w_1^2 - 1)^{3/2} w_o^2} \tag{60}$$

$$\mathrm{Im}\left(\frac{(k^2 D_e^2 + W_e) Z W_i T_c / T_i}{k^2 D_e^2 + W_e + Z T_e W_i / T_i}\right) .$$

The angle ϕ which gives maximum amplification is given by

$$\cos\phi = \frac{(w_o^2 - 1)^{1/2} - (w_o^2 - w_1^2)^{1/2}}{(w_1^2 - 1)^{1/2}} \tag{61}$$

and, as a rule, $\cos\phi$ has the value ≈ 0.5 for maximum amplification. Physically, the angular optimization represents a tradeoff between maximizing $\gamma(\phi \to 90°)$ and minimizing $V_{g\xi}$ $(\phi \to 0°)$.

Next, let us relate E_o^2 to the imput power from a waveguide port. The dimensions of the waveguide port are taken to be L in the direction along the magnetic field and $3\lambda_o/4$ in the y-direction, λ_o being the vacuum wavelength associated with ω_o. Combining the formula for the energy density of a lower hybrid wave,

$$U = (E_o^2/8\pi)[1 + (\omega_{pe}^2/\Omega_e^2)] \quad , \tag{62}$$

with the group velocity, etc., one computes the relation between the power-per-port P and the value of E_o^2 in one of the two resonance cones which eminate from the port to be

$$\frac{P}{2} = UL\ (\tfrac{3}{4}\lambda_o)\ V_{go,x}(\tfrac{r}{a}) \quad , \tag{63}$$

where a/r is a cylindrical focussing factor appropriate to tokamaks, and

$$V_{go,x} = \frac{c}{n_z}\ \frac{(w_o^2 - 1)^{3/2}}{w_o^2}\ (\tfrac{Zm}{M})^{1/2} \quad . \tag{64}$$

Here n_z denotes the parallel phase velocity generated by the phased waveguide array. Finally, one can use (10) to relate L_ξ to L

$$L_\xi = \frac{1}{\sqrt{2}}\ L\left(\frac{Zm}{M}\right)^{1/2}\left(w_o^2 - 1\right)^{1/2} \quad , \tag{65}$$

combine (60) - (65), use (7) to relate $k_{\perp 1}$ to $k_{\|1}$, and obtain

$$A = n_z(P/P_o)\ A(w_o, w_1) \tag{66}$$

where

$$P_o = \frac{3}{2}\left(1 + \frac{\omega_{pe}^2}{\Omega_e^2}\right)^2\ \frac{B^2}{\omega_{pi}^2}\ (\tfrac{r}{a})\left(\frac{ZT_e}{M}\right)^{3/2} \quad , \tag{67}$$

$$A(w_o,w_1) = \frac{w_o w_1^3 [(w_o^2-1)^{1/2} - (w_o^2-w_1^2)^{1/2}]}{(w_o^2-1)(w_1^2-1)^2 V_e} B \tag{68}$$

$$B = \mathrm{Im}\left(\frac{-(k^2 D_e^2+W_e) ZWT_e/T_i}{k^2 D_e^2+W_e+ZT_e W_i/T_i} \right) \tag{69}$$

and

$$V_e = (\omega_1/k_{||})(m/T_e)^{1/2} \quad .$$

Formula (66) has been cast so as to be most useful in the low density region near the edge of the plasma when ω_o, $\omega_1 >> \omega_{LH}$. Here the principal damping of daughter waves is via electron-Landau damping and one must require that V_e be sufficiently large to avoid serious damping. A direct calculation of the linear spatial damping e^{-S} suffered by the daughter wave combines (13), (56), (61), and (65) into the result

$$S = \frac{\gamma_L T_\xi}{V_g \xi} = \frac{\pi}{2}^{3/2} \left(\frac{mc^2}{T_e}\right)^{1/2} \frac{(w_o^2-1)^{1/2}(w_1^2-1)^{3/2} V_e^2 \exp(-V_e^2/2)}{w_o (w_o^2-w_1^2)^{1/2}} \quad , \tag{70}$$

where

$$L = \lambda_o/2 \quad ,$$

was employed to estimate the size of the waveguide launching structure (Fig. 1). Evidently, $V_e > 4$ assures negligible spatial damping, while for $V_e < 4$, the damping is appreciable. Consequently, the amplification can be estimated with good accuracy by using $V_e = 4$ in formula (68).

In the low-density region near the edge of a tokamak, the local lower hybrid frequency is quite low so that $\omega_o, \omega_1 >> \omega_{LH}$. The principal low-frequency coupling is then via ion sound waves and the maximum of the coupling function B occurs when

$$(\omega_1 - \omega_o)^2 \approx \frac{k_\perp^2 (ZT_e + 3T_i)}{M} \quad . \tag{70}$$

The actual maximum value of B depends strongly on the effective temperature ratio ZT_e/T_i. When $ZT_e/T_i < 3.5$, the real part of the denominator of (69) never vanishes and true ion-acoustic waves do not exist. In this regime, the maximum value of B depends strongly on temperature ratio as Fig. 6 shows. In the opposite case $ZT_e/T_i > 3.5$, the maximum value of B is determined by the electron-Landau damping contribution to W_e, which can be expressed as

$$W_e \approx 1 + i \left(\frac{\pi m}{2T_e}\right)^{1/2} \left(\frac{\omega_o - \omega_1}{k_{||}}\right) \approx 1 + i \left(\frac{\pi}{2}\right)^{1/2} \left(1 + \frac{3T_i}{ZT_e}\right)^{1/2} \frac{1}{(w_1^2 - 1)^{1/2}} \tag{71}$$

In this limit, one finds that

$$\max B = \left(\frac{2}{\pi}\right)^{1/2} \frac{(w_1^2 - 1)^{1/2}}{(1 + 3T_i/ZT_e)^{1/2}} \quad . \tag{72}$$

The frequency shift $\omega_o - \omega_1$ may be computed using (71), (68), and dispersion relation (7). The result is

$$\omega_o - \omega_1 = \frac{\omega_1}{V_e}\left(1 + \frac{3T_i}{ZT_e}\right)^{1/2} \frac{\omega_{LH}}{(\omega_1^2 - \omega_{LH})^{1/2}} \sim \frac{\omega_{LH}}{V_e}\left(1 + \frac{3T_i}{ZT_e}\right)^{1/2} \omega_1 >> \omega_{LH} \quad . \tag{73}$$

For the modes with maximum amplification, one takes $V_e \approx 4$ and finds that the frequency shift is a good fraction of the local lower hybrid frequency.

Figures (7) and (8) present the results of a computational evaluation of (68) maximized over wave number for fixed ω_o, ω_1. The linear damping decrements, which we dropped following (57), were reinstated to obtain a maximum. As Figs. (7) and (8) show, the maximum amplification occurs for $V_e \approx 4$ and $\cos\phi \approx .5$, in agreement with our values for V_e and $\cos\phi$. When w_o is large, the combination of (66), (68), and (72) leads to

$$\max_{w_1} A = n_z \frac{P}{P_o} \left(\frac{2}{\pi}\right)^{1/2} \frac{\cos\phi_m}{V_e(1 + 3T_i/ZT_c)^{1/2}} \quad , \tag{74}$$

where $\cos\phi_m$ is the value of Eq. (61) at maximum amplification. Let us estimate that instabilities will occur when max A > 6. This condition implies that there is a threshold power P_{th} for convective instabilities to occur in the low density regions

$$P > P_{th} = \frac{9(\pi/2)^{1/2} V_e}{n_z \cos\phi_m}\left(1 + \frac{3T_i}{ZT_e}\right)^{1/2} \left(\frac{r}{a}\right) \frac{B^2}{\omega_{pi}^2}\left(\frac{ZT_e}{M}\right)^{3/2} \tag{75}$$

$$= (3.1 \text{ Megawatts}) \cdot \left(\frac{Z}{A}\right)^{1/2} \frac{V_e}{n_z} \left(1 + \frac{3T_i}{ZT_e}\right)^{1/2} \left(\frac{r}{a}\right) \qquad (76)$$

$$\left(\frac{B}{50kG}\right)^2 \left(\frac{T_e}{100eV}\right)^{3/2} \left(\frac{10^{12}\,cm^{-3}}{n_e}\right)$$

where Z and A are the atomic number and mass of the plasma ion. Evidently, instabilities will break out first where the quantity $(Z/A)^{1/2} T_e^{3/2} n_e^{-1} (r/a)$ has a minimum value.

In higher density regions, the lower hybrid frequency begins to become comparable with the pump frequency, and Fig. (8) shows that the threshold power decreases because A becomes larger than its asymptotic value.

Special consideration must be given to the case where the daughter wave frequency is close to the lower hybrid frequency and an apparent divergence occurs in (68). As is well known, linear mode conversion processes constrain the daughter wave frequency to be a finite amount above the lower hybrid frequency

$$w_1 - 1 > \sqrt{3}(T_i/Z_m)^{1/2}(k_{\|1}/\omega_1) = \sqrt{3}\,(T_i/ZT_e)^{1/2}(1/V_e) \cdot \qquad (77)$$

Furthermore, it is clear that the inequality $k_{\|1} > k_{\|o} = n_z\omega_o/c$ must hold in order that waves be localized within the resonance cone of the pump. This leads to

$$w_1 - 1 > \sqrt{3}\, n_z w_o (T_i/mc^2)^{1/2} \sim 0.1 \qquad (78)$$

and removes the apparent divergence. Consequently, our plots contain entries only for $w_o, w_1 > 1.1$.

It is instructive to employ the relationship between the pump electric field and the incident power (62) - (64) to transform the threshold criterion for absolute modes in low density regions ($w_o >> 1$) into

$$P > P_A = \left(\frac{3|\Lambda_2|}{2}\right)\left(\frac{v_e}{n_z}\right)\left(1 + \frac{T_i}{ZT_e}\right)\left(\frac{r}{a}\right)\frac{B^2}{\omega_{pi}^2}\left(\frac{ZT_e}{M}\right)^{3/2}\frac{(w_o^2-1)^2}{w_o^3} \qquad (79)$$

with $|\Lambda_2|$ given by Fig. (4). A comparison with the corresponding formula (75) for quasimode decay instabilities points out that, the threshold for absolute modes is comparable to or less than the threshold for decay instabilities, but depends on the frequency w_o.

Overall, the key feature which a spatially localized pump produces is that the low phase velocity daughter waves undergo the largest convective amplification by dint of their low group velocity. Only linear damping processes prevent very small phase velocities and correspondingly large amplifications. Low-phase velocity waves have large wavenumbers and generate a substantial frequency shift between the pump and daughter lower hybrid waves [see (73)].

V. TOKAMAK APPLICATIONS

Efficient heating of tokamak plasmas has become one of the key objectives of controlled fusion reserach. Out of the variety of heating schemes proposed, only lower hybrid heating offers the dual advantages of an established technology for power generation and a particularly simple waveguide method for introducing power into the plasma. But experimental attempts[2,3] to heat plasmas via lower hybrid radiation have raised serious questions concerning whether nonlinear processes absorb the energy at the plasma periphery. The principal application of this paper is to show how to avoid nonlinear absorption mechanisms. A companion paper addresses the question of the nonlinear saturation of lower hybrid instabilities and the consequent nonlinear absorption of the pump wave, which will be serious for large tokamaks.

Our most significant conclusion pertains to the threshold for parametric instabilities in the low density periphery where the frequency is several times the local lower hybrid frequency. Threshold formulas (76) and (79) show that the threshold is in the regime of current tokamak experiments, and that nonlinear effects can be suppressed by high toroidal field, low-density and high-electron temperatures. Furthermore, if $ZT_e/T_i < 3.5$, the frequency dependence shown in Figs. (6-8) and in (79) predicts that the threshold power increases linearly with applied frequency. When $ZT_e/T_i > 3.5$, ion-acoustic waves exist and there is no explicit frequency dependence of the threshold as (74) makes clear.

It is difficult to apply our results to real tokamaks because not much is known regarding the temperature and density profiles in the periphery of actual devices, and partially ionized impurities also serve to reduce the threshold field. But the threshold conditions do predict that an increase in electron temperature generated by nonlinear heating will quench parametric instabilities. High-power, lower hybrid radiation may suppress severe absorption near the surface of a tokamak merely by raising the electron temperature by a modest amount of nonlinear absorption.

The most straightforward way to eliminate nonlinear effects is to introduce the requisite power through a number of waveguide ports, thereby reducing the peak electric field in the resonance cone associated with a particular waveguide. No mutual coupling occurs between resonance cones because of the strong spatial attenuation of the daughter waves due to their low-phase velocity.

What about other methods to suppress parametric instabilities? Convective decay instabilities will not be controlled by a finite bandwidth of the pump wave unless this bandwidth is as large as the characteristic frequency shifts (73) - typically 10% of the pump frequency. The stabilization of absolute instabilities can be effected by smaller bandwidths comparable to the frequency shifts of the daughter waves (53) - perhaps 5% of the pump frequency. High toroidal fields are doubly beneficial; not only do they increase the threshold field for parametric instabilities, but also the energy confinement improves thereby reducing the power required for heating.

Although instabilities may be eliminated near the plasma periphery, Figs. (6-8) clearly indicate that the threshold for parametric instabilities falls by one or two orders of magnitude as the lower hybrid layer is approached. Hence, nonlinear absorption will probably attenuate the pump wave before it reaches the linear mode conversion surfaces.

Our second key result concerns the fate of the energy transferred to the daughter waves. These waves rapidly propagate out of the resonance cone region where they are no longer unstable and are absorbed by Landau damping with electrons of energy roughly $8T_e$ playing the principal role. Since the frequency shift of the daughter wave remains a small (but not completely negligible) fraction of the pump frequency, and since quasimode coupling conserves plasmon number, most of the energy transferred out of the pump wave goes to the lower hybrid daughter wave. One concludes that nonlinear lower hybrid heating will proceed via the formation of an energetic tail in the parallel velocity distribution. Two recent experiments corraborate this expectation[2,12].

If the formation of parallel velocity tails serves to increase the fraction of the plasma current carried by runaway electrons, lower hybrid heating could cause a reduction in the Ohmic heating of a tokamak. Such an effect would clearly be observed on the loop voltage record. Since runaways are to be avoided, the pump lower hybrid radiation would best be a travelling wave propagating in a direction opposite to that of runaway electrons (i.e. propagating with the plasma current). The parallel velocity tail formed by the linear damping of the pump wave would then consist of anti-runaways and would increase the Ohmic heating.

Experiments have also shown the formation of energetic ion tails, raising the question: When is ion heating expected? The answer is that nonlinear ion heating can occur in two ways. First, ion-Landau damping provides part of the dissipation in quasimodes, and the energy associated with the quasimode can be transferred to partially to ions. The remainder of the quasimode energy goes to electrons. Indeed, according to the model of this paper, if $ZT_e/T_i > 3.5$, then the quasimode dissipation is dominantly electron-Landau damping and very little energy is transferred to the ions. However, the plasma in the outside regions of a tokamak is not a single species plasma, but is composed of partially ionized impurities plus hydrogen or deuterium. Impurities lower the sound speed so that Landau damping by the hydrogen isotopes becomes important, and hydrogen can be energized directly. Concomitantly, there will be little direct heating of impurity ions because their velocities are less than that of hydrogen. Nonlinear ion heating also occurs when the daughter wave frequency ω_1 satisfies $\omega_1 < \omega_{LH}(1+T_i/ZT_e)^{1/2}$ and the principal damping process changes from electron to ion-Landau damping. Again, a multiple species plasma will differ from our simple model. Hence, we conclude that nonlinear absorption near the linear mode conversion surface will heat the lightest ions.

Our model of a spatially localized pump leads directly to the prediction that the frequency shift [Fig. 8 and (73)] is about 10% of the pump frequency in agreement with experimental results.[3]

Next, let us briefly argue that decay into two lower hybrid modes will not play an important role. The paper by Ott[13] compares the threshold for quasimode decays versus that for decay into two lower hybrid modes. Transferring his Eq. (13a) into our notation, one obtains

$$\frac{P_{\text{quasimodes}}}{P_{\text{decay}}} \sim n_z^2 \left(\frac{T_e}{mc^2}\right)^{1/2} \frac{2L}{\lambda_o} \frac{w_1}{w_1^2 - 1} \left(\frac{\pi}{V_e}\right) << 1 \quad , \tag{80}$$

where w_1 is the frequency of the daughter decay wave, and the convective damping decrement was estimated as $\nu \sim V_{g||}/L$. The principal reason why decay into two lower hybrid modes fails to be important is that it depends on the finite wavelength of the pump. In the nonlinear saturation of growing short wavelength daughter waves, the decay into two other waves could well play an important role.

Parametric instabilities can also occur for very large phase velocity waves which can transit several times around the torus before damping. Equation (73) points out that such instabilities will be characterized by a very small frequency shift. When translated into energy, this means that essentially all the energy transferred out of the pump appears in the daughter wave, so that a true absorption process has not taken place. On the other hand, the daughter wave vector will be directed principally in the short azimuthal direction, so that the daughter wave propagates much more slowly to the center, and may even return to the outside due to the magnetic shear effects.

As an estimate for the threshold of high phase velocity waves, let us set the growth rate (57) equal to the collisional damping rate and take E_o^2 to be the average electric field in the torus.

$$\frac{E_o^2}{8\pi}\left(1 + \frac{\omega_{pe}^2}{\Omega_e^2}\right) 4\pi^2 RrV_{gr} = P \quad .$$

The threshold condition then becomes $P > P_o$ with

$$P_o = \left(\frac{B^2}{\omega_{pi}^2}\right)\left(\frac{r}{a}\right)\sqrt{\frac{\pi}{2}}\ \frac{1}{n_z}\left(\frac{ZT_e}{M}\right)^{3/2}\left[\left(\frac{\nu_e 2\pi R}{\bar{V}_c}\right)\left(\frac{2\pi a}{\lambda_o}\right)\left(\frac{w_o^2 - 1}{w_o^2}\right)\right.$$

$$\left.\cdot\left(\frac{\omega_{pe}^2}{\Omega_e^2 + \omega_{pc}^2} + \frac{w_o^2 - 1}{w_o^2}\right)\left(1 + \frac{\omega_{pe}^2}{\Omega_e^2}\right)^2\right] \qquad (81)$$

$$= \frac{(2\pi)^2}{3}\ \frac{B^2 e^2 Rr\ell n\Lambda}{T_e^{\frac{1}{2}}\lambda_o}\left(\frac{Z}{M}\right)^{1/2}\left(\frac{w_o^2 - 1}{w_o^2}\right)\left(1 + \frac{\omega_{pe}^2}{\Omega_e^2}\right)^2\left(\frac{\omega_{pe}^2}{\Omega_e^2 + \omega_{pe}^2} + \frac{w_o^2 - 1}{w_o^2}\right)$$

where (72) has been used.

Equation (81) has been written to facilitate comparison with (75). For present-day tokamaks, one can estimate that the factor in $[\ ]$ brackets in much less than unity so that the threshold for high-phase velocity waves is much lower than convective quasimodes in the peripheral region. Casting (81) into practical units, one obtains the threshold condition

$$P > P_o = (100 \text{ kilowatts}) \left(\frac{100eV}{T_e}\right)^{1/2} \left(\frac{B}{50kG}\right)^2 \left(\frac{r}{\lambda_o}\right) \frac{1}{n_z} \left(\frac{w_o^2 - 1}{w_o^2}\right) \left(\frac{Z}{A}\right)^{1/2} \cdot \left(1 + \frac{\omega_{pe}^2}{\Omega_e^2}\right)^2 \left(\frac{\omega_{pe}^2}{\Omega_e^2 + \omega_{pe}^2} + \frac{w_o^2 - 1}{w_o^2}\right) \tag{82}$$

where $\ell n\Lambda \approx 20$ was used. Evidently high-phase velocity waves become unstable at quite low powers. On the other hand, high-phase velocity instabilities are not a major obstacle to tokamak heating because the nonlinear coupling rates are of the order of the collision frequency. Hence, the effective collision frequency for the pump wave caused by the instabilities will also be of the order of the collision frequency and not important in the absorption of the pump wave. Experimental results on the ATC Tokamak show instabilities slightly below the pump frequency as (82) predicts.

Another possibly important effect remains to be investigated: scattering of lower hybrid radiation by drift-wave irregularities in the plasma periphery. The lower hybrid dispersion relation can be written as

$$k_\perp \rho_i = n_z \left(\frac{\beta_i M}{2Zm}\right)^{1/2} \frac{\omega_o}{(\omega_o^2 - 1)^{1/2}} , \tag{83}$$

which shows that $k_\perp \rho_i \lesssim 1$ for typical tokamak discharges. Hence, lower hybrid waves could scatter off of drift wave turbulence. Since drift waves generally have a much longer parallel wavelength than lower hybrid waves, and a very much lower frequency,

the scattering process will simply result in a reorientation of the perpendicular wave vector. With frequent scattering, the lower hybrid waves will penetrate a tokamak only by a diffusive random walk process.

The attenuation length caused by scattering can be computed by starting with Eq. (11) rewritten as

$$(k'^2 - k_o^2)\,\phi_{\underset{\sim}{k}'} = -i\,\frac{\omega_o}{\Omega_i}\,\frac{1}{(w_o^2-1)}\,\underset{\sim}{k}'\cdot(\underset{\sim}{k}_o\times\underset{\sim}{z})\,\frac{n_{\underset{\sim}{k}''}}{n}\,\phi_{\underset{\sim}{k}_o} + \frac{2\omega_o k_o^2}{\omega_{LH}^2(w_o^2-1)}\,\frac{\partial}{\partial\tau}\,\phi_{\underset{\sim}{k}'} \quad . \tag{84}$$

This equation gives the evolution with time τ (we used $-i\omega+\bar{\gamma}\to\partial/\partial\tau$) of the amplitude $\phi_{\underset{\sim}{k}'}$ scattered from the incident wave $\phi_{\underset{\sim}{k}_o}$ by the dc density fluctuation $n_{\underset{\sim}{k}''}$, ($\underset{\sim}{k}'' = \underset{\sim}{k}' - \underset{\sim}{k}_o$). Since $\underset{\sim}{k}'' = 0$, we consider wave vector components only in the two dimensions transverse to the magnetic field. Defining $k'^2 = k_o^2 + 2k_o\delta k$, one can obtain the equation

$$\frac{\partial\phi_{\underset{\sim}{k}'}}{\partial\tau} + i\delta k\,\frac{\partial\omega}{\partial k_\perp}\,\phi_{\underset{\sim}{k}'} = \frac{\omega_{LH}^2}{2\Omega_i}\sin\theta\,\frac{n_{\underset{\sim}{k}''}}{n}\,\phi_{\underset{\sim}{k}_o} \tag{85}$$

where $\sin\theta = \underset{\sim}{k}'\cdot(\underset{\sim}{k}_o\times\underset{\sim}{z})/k_o^2$.

This equation can be treated via the usual perturbation methods of quantum mechanics to obtain the scattering frequency ν_s.

$$\nu_s = \frac{1}{\tau}\sum_{\underset{\sim}{k}'}\left|\frac{\phi_{\underset{\sim}{k}'}}{\phi_{\underset{\sim}{k}_o}}\right|^2 = \frac{\pi^2}{2}\,k_o\,\left(\frac{\partial k_\perp}{\partial\omega}\right)\,\frac{\omega_{LH}^4}{\Omega_i^2}\,\frac{\langle|\Delta n(\underset{\sim}{k}'')|^2\rangle}{n^2} \tag{86}$$

Next, we will approximate the power spectral density in $\underset{\sim}{k}$-space $\langle|\Delta n(\underset{\sim}{k}'')|^2\rangle$ by $(\Delta n)^2/\pi k_o^2 \approx \langle|\Delta n(\underset{\sim}{k}'')|^2\rangle$ - a formula which assumes that most of the naturally occurring density fluctuations have wave numbers ~ k_o. With the help of (55), one obtains the characteristic distance for attenuation by scattering

$$\ell_s = \frac{V_{g\perp}}{\nu_s} = \frac{2}{\pi}\frac{(w_o^2-1)^2}{k_o w_o^2}\frac{\Omega_i^2}{\omega_{LH}^2}\frac{n^2}{(\Delta n)^2} = \frac{\lambda_o}{\pi^2}\left(\frac{M}{Zm}\right)^{-1/2}\frac{(w_o^2-1)^{5/2}}{n_z}\frac{\Omega_i^2}{\omega_o^2}\frac{n^2}{(\Delta n)^2} \quad (87)$$

This scattering length is generally long in the tenuous periphery of the plasma (assuming $\Delta n/n \sim 10^{-2}$), but can become short in the high-density regions because of the strong scaling with density ($\ell_s \propto n^{-5/2}$ for fixed $\Delta n/n$). Scattering, then, plays a negligible role in lower hybrid heating.

Magnetic shear will influence the propagation of long-wavelength daughter waves which transit many times around the torus. But since we have argued following Eq. (82), that such waves will not constitute an important absorption process, magnetic shear will be neglected.

Overall, our assessment is that parametric instabilities place an important limit on the power-per-port that a lower hybrid heating scheme can employ [c.f. (70)]. The experience of present-day tokamaks will most likely be quite relevant to fusion reactors, because they too must have low-temperature, low-density regions on the outside. Parametric instabilities may be avoided by high toroidal field and many separate wave-launching ports. Also, launching the electromagnetic whistler mode, instead of the

slow electrostatic wave as assumed in this work, may well lead to superior heating. The whistler has a higher perpendicular group velocity, thereby lowering the pump electric field. Furthermore, it is a global mode and does not possess a resonance cone structure.

ACKNOWLEDGEMENTS

We have benefited from disucssions with S. Bernabei, W. Hooke, G. Morales, R. Motley and M. Porkolab.

This work was supported by U.S. Research and Development Administration Contract No. E(11-1)-3073.

REFERENCES

[1]M. Brambilla, Nucl. Fusion 16, 47 (1976).

[2]V. V. Alikaev, Yu. I. Arsen'ev, G. A. Bobrovskii, V. I. Poznyak, K. A. Razumoua, and Yu. A. Sokolov, Zh. Tekh. Fiz. 45, 523 (1975) [Sov. Phys. Tech. Phys. 20, 327 (1975)].

[3]W. M. Hooke, Bull. Am. Phys. Soc. 20, 1313 (1975); M. Porkolab, Bull. Am. Phys. Soc. 20, 1313 (1975).

[4]M. Porkolab in Symposium on Plasma Heating in Toroidal Devices, Varenna, 1974 (Editrice Compositori, Bologna, 1974)p. 41.

[5]M. Porkolab, Phys. Fluids 17, 1432 (1975).

[6]G. Hasselberg, and A. Rogister, Phys. Fluids 19, 108 (1976).

[7]G. J. Morales and Y. C. Lee, Phys. Rev. Letters 35, 930 (1975).

[8]W. Gekelman and R. L. Stenzel, Phys. Rev. Letters 35, 1708 (1975).

[9]K. Nishikawa and C. S. Liu, in Advances in Plasma Physics, Vol. 6 (John Wiley, New York, 1976)p. 1.

[10]R. J. Briggs and R. R. Parker, Phys. Rev. Letters 29, 852 (1972).

[11]P. M. Bellan and M. Porkolab, Phys. Fluids 17, 1592 (1974).

[12]D. A. Boyd, F. J. Stauffer, and A. W. Trivelpiece, Phys. Rev. Letters 37, 98 (1976).

[13]E. Ott, Phys. Fluids 18, 566 (1975).

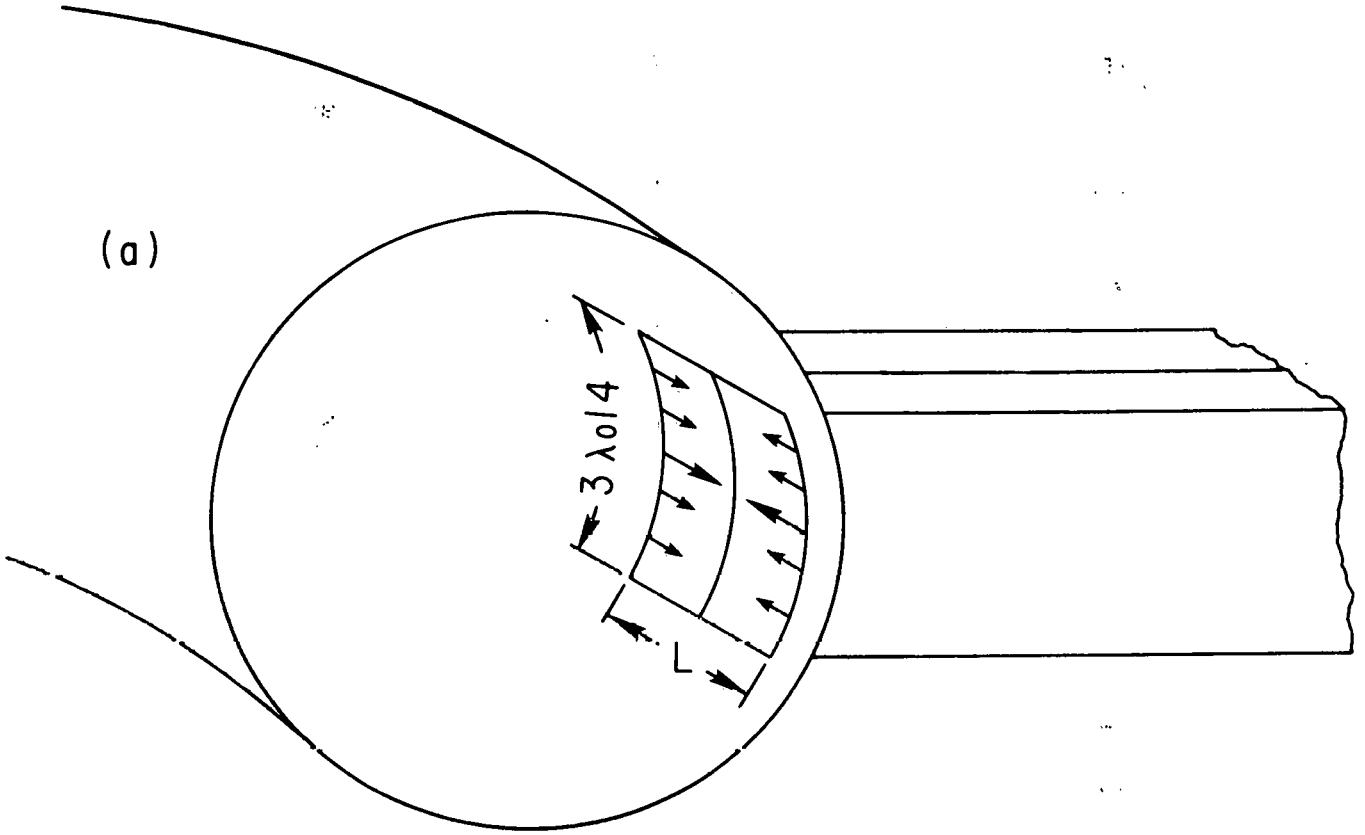

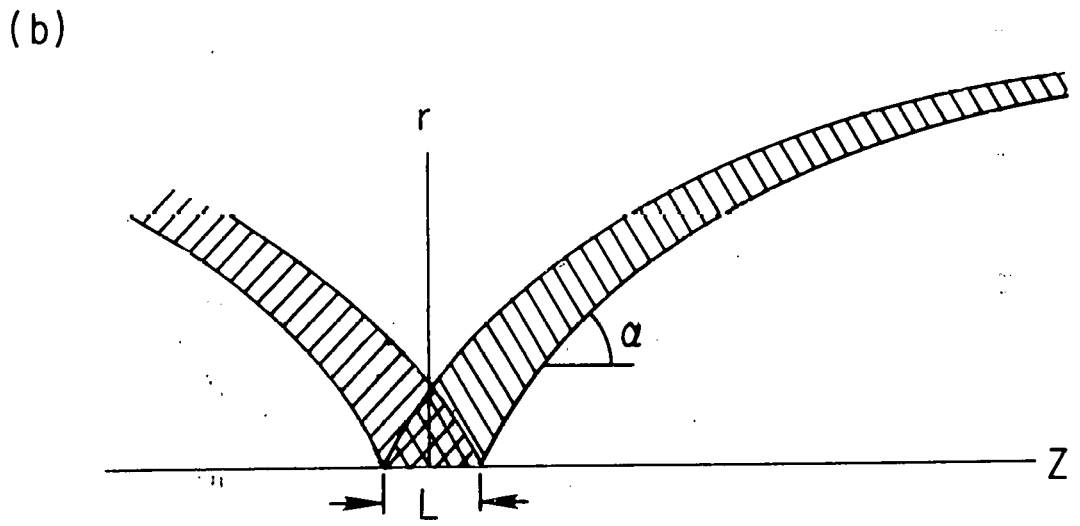

762202

Fig. 1(a). Sketch of two element phased array waveguide coupler in a tokamak. The electric field vectors are out of phase. L is the total length along the magnetic field. (b) Sketch of resonance cone propagation in minor radius r and distance along the magnetic field z.

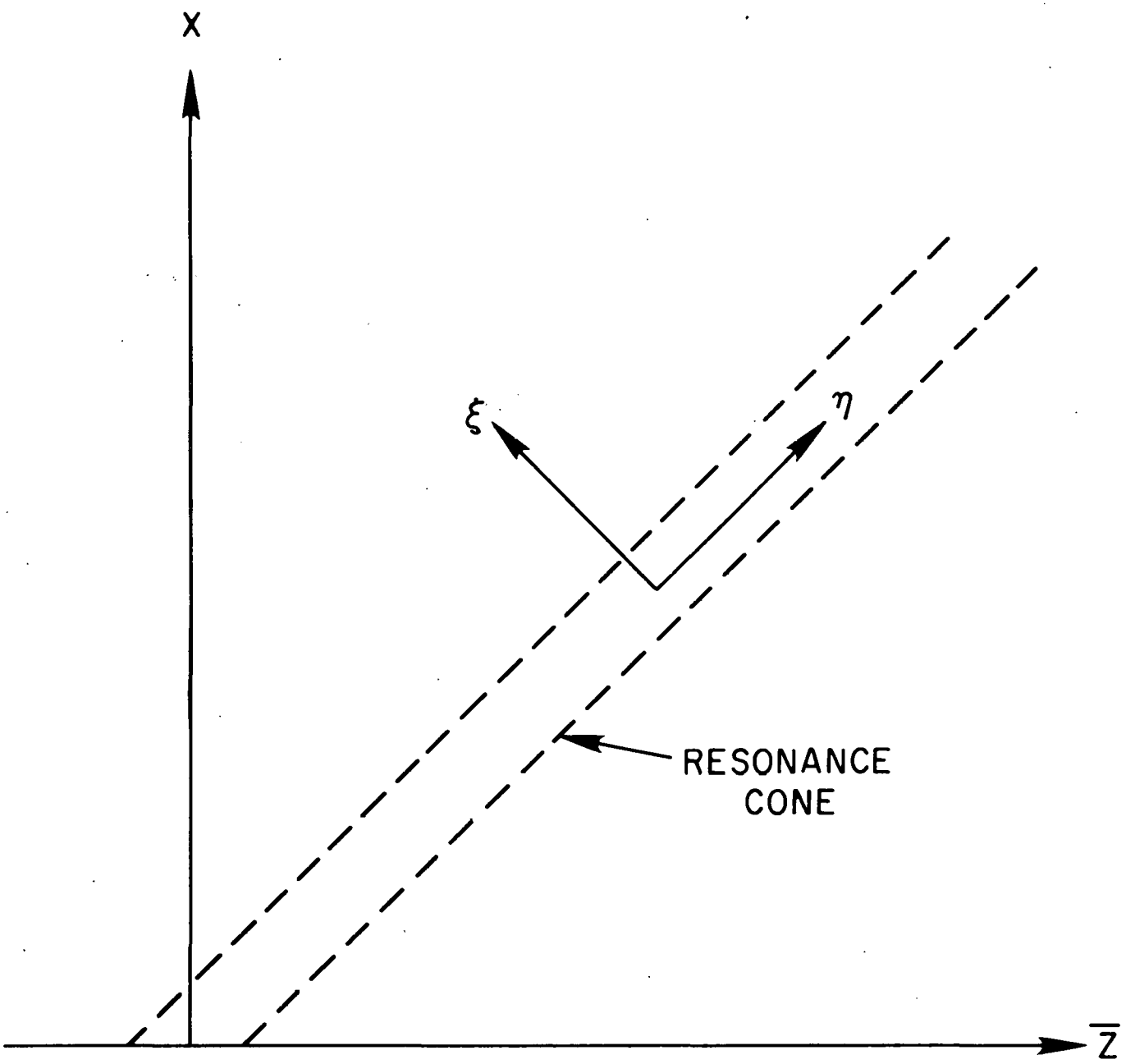

762197

Fig. 2. The resonance cone lies at 45^{o} in terms of the scaled variable $\bar{z}$ [see Eq. (14)]. The ξ,η coordinate system is defined by (16).

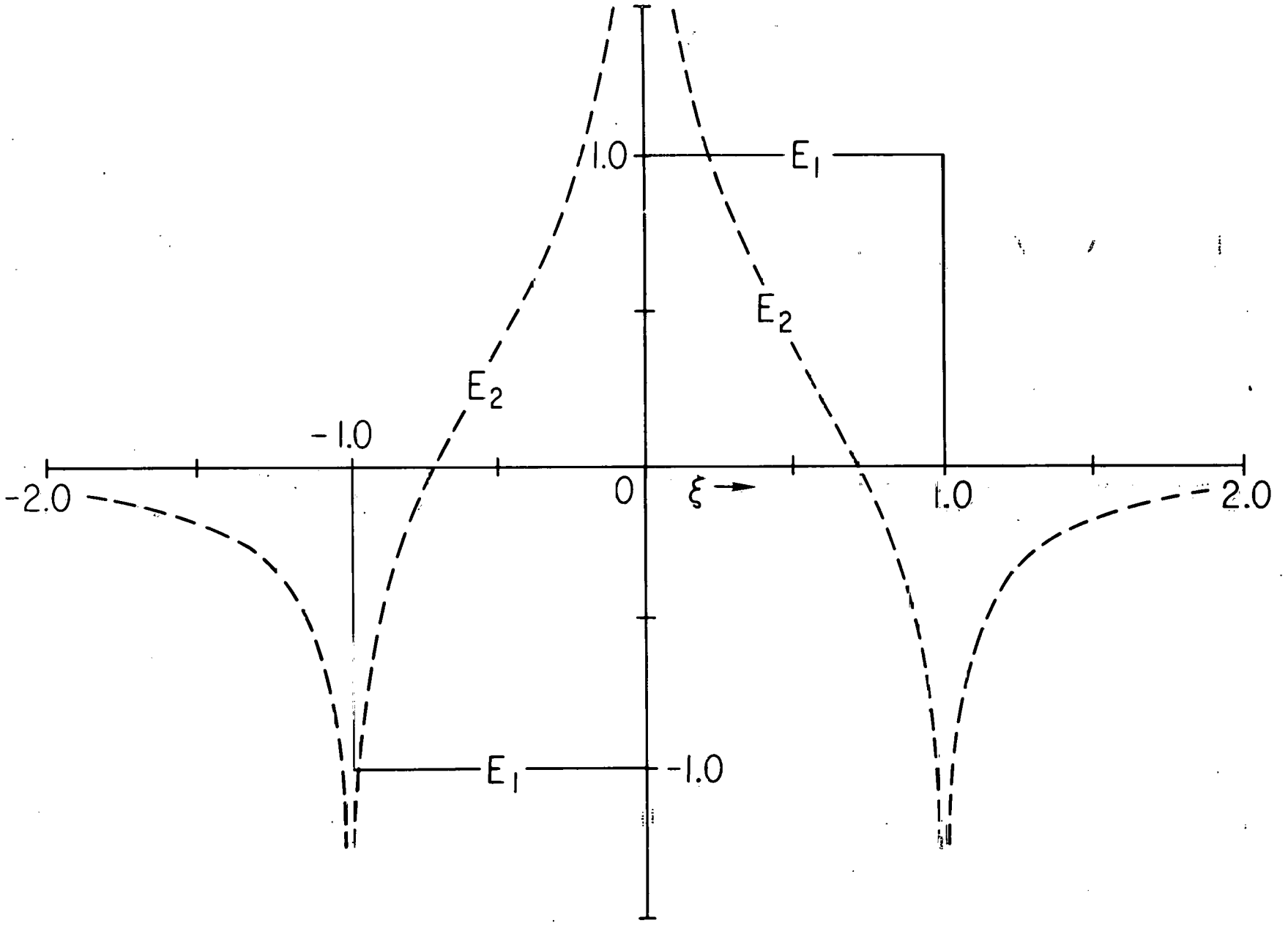

Fig. 3. The electric field amplitudes E_1 and E_2 corresponding to the $\cos\omega_o t$ and $\sin\omega_o t$ components respectively [see Eq. (17, 18)]. These amplitudes model the resonance cone fields generated by the waveguide coupler in Fig. 1.

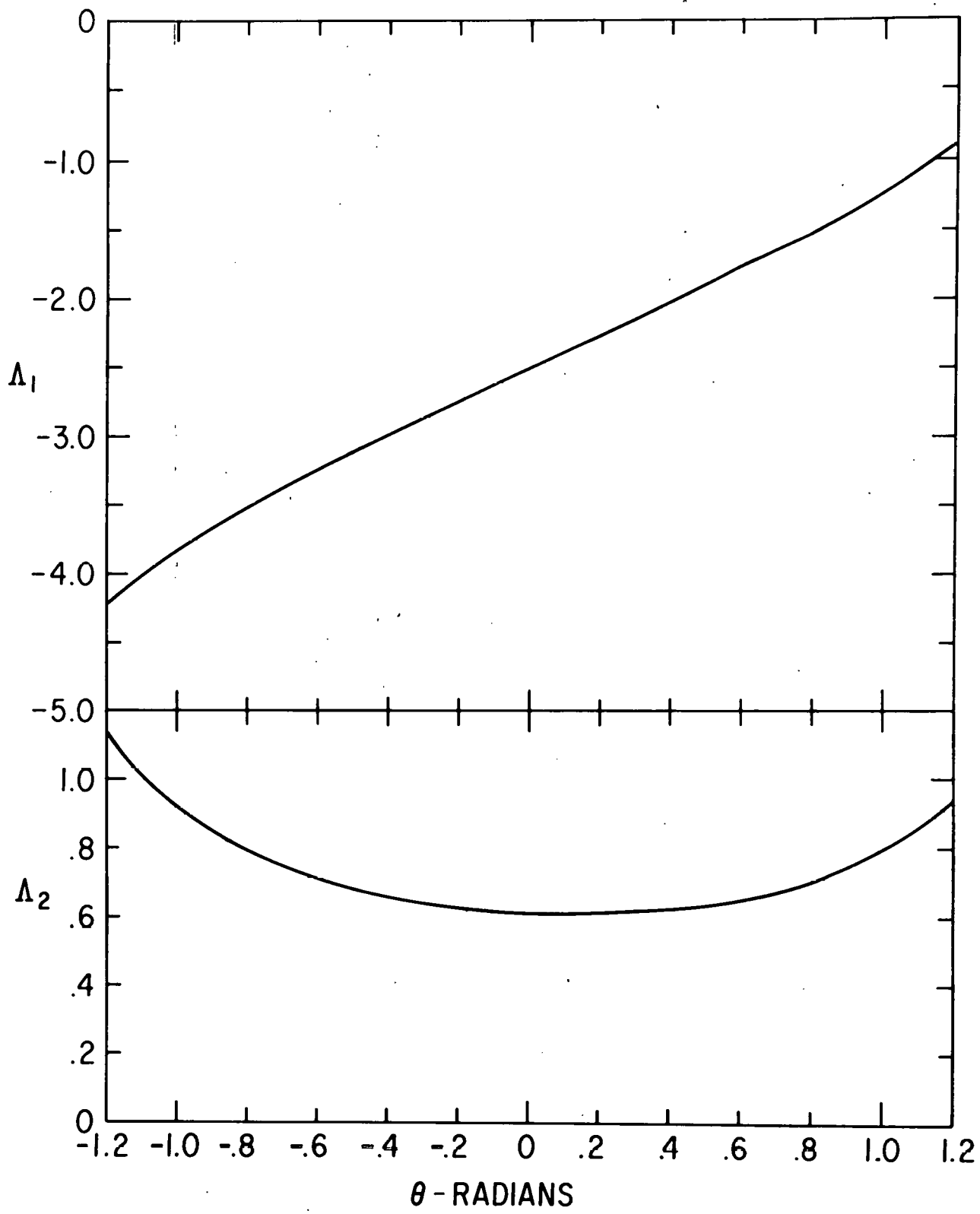

Fig. 4. Results of computational solutions for the eigenvalue pair $(\Lambda_1, |\Lambda_2|)$ of Eqs. (45), (52) in terms of the parameter which is related to ion Landau damping dissipation via (42). As $|\theta| \to \pi/2$, solutions to (45) cease to exist.

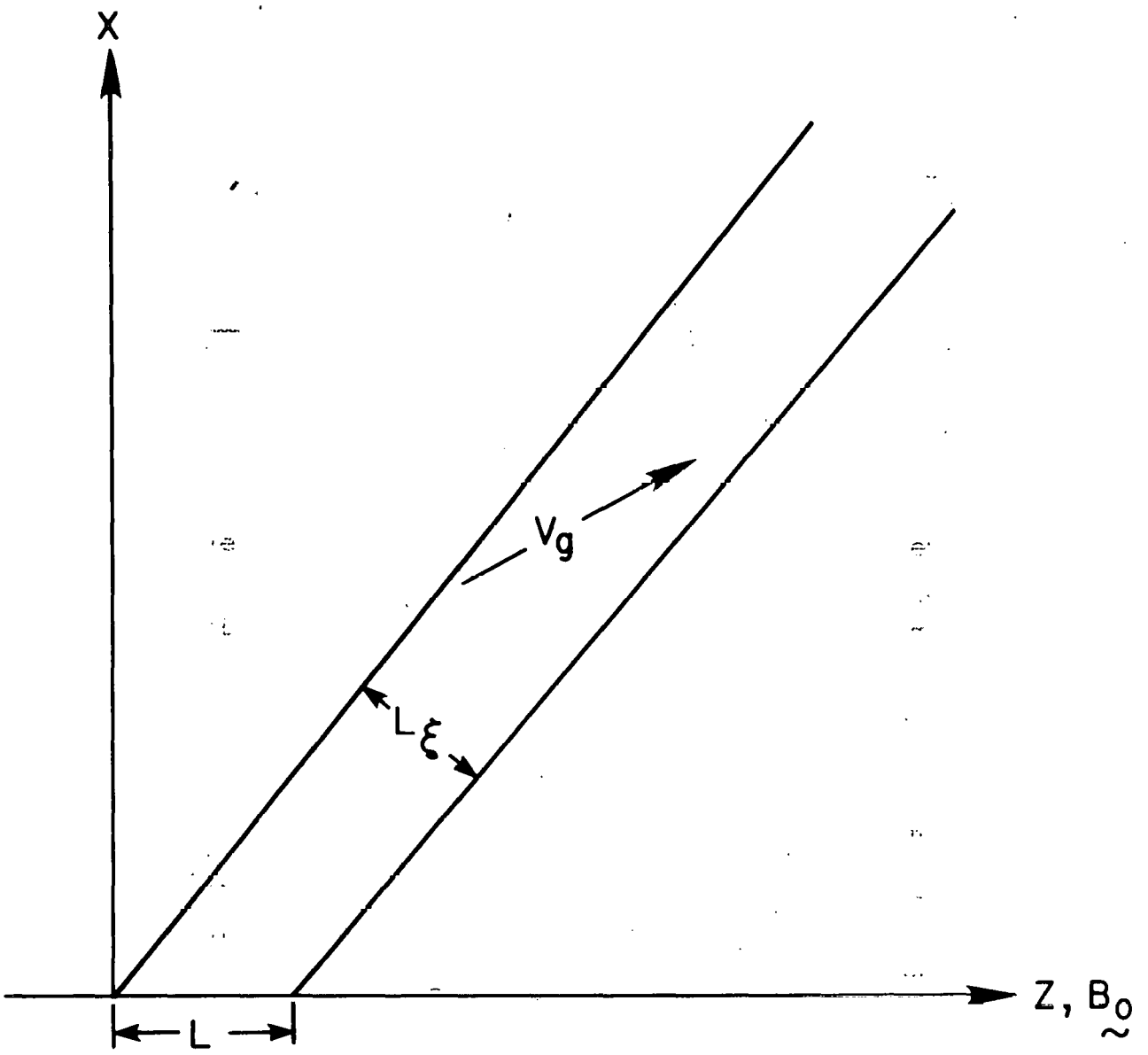

762199

Fig. 5. Geometry of the quasimode amplification process. The pump wave propagates in the well-defined resonance (whose angle with respect to the B_o - direction is greatly exaggerated). The component of the daughter wave group velocity in the x-z plane is sketched. [See (56) for the precise formula]. L is the dimension of the waveguide launcher along the magnetic field.

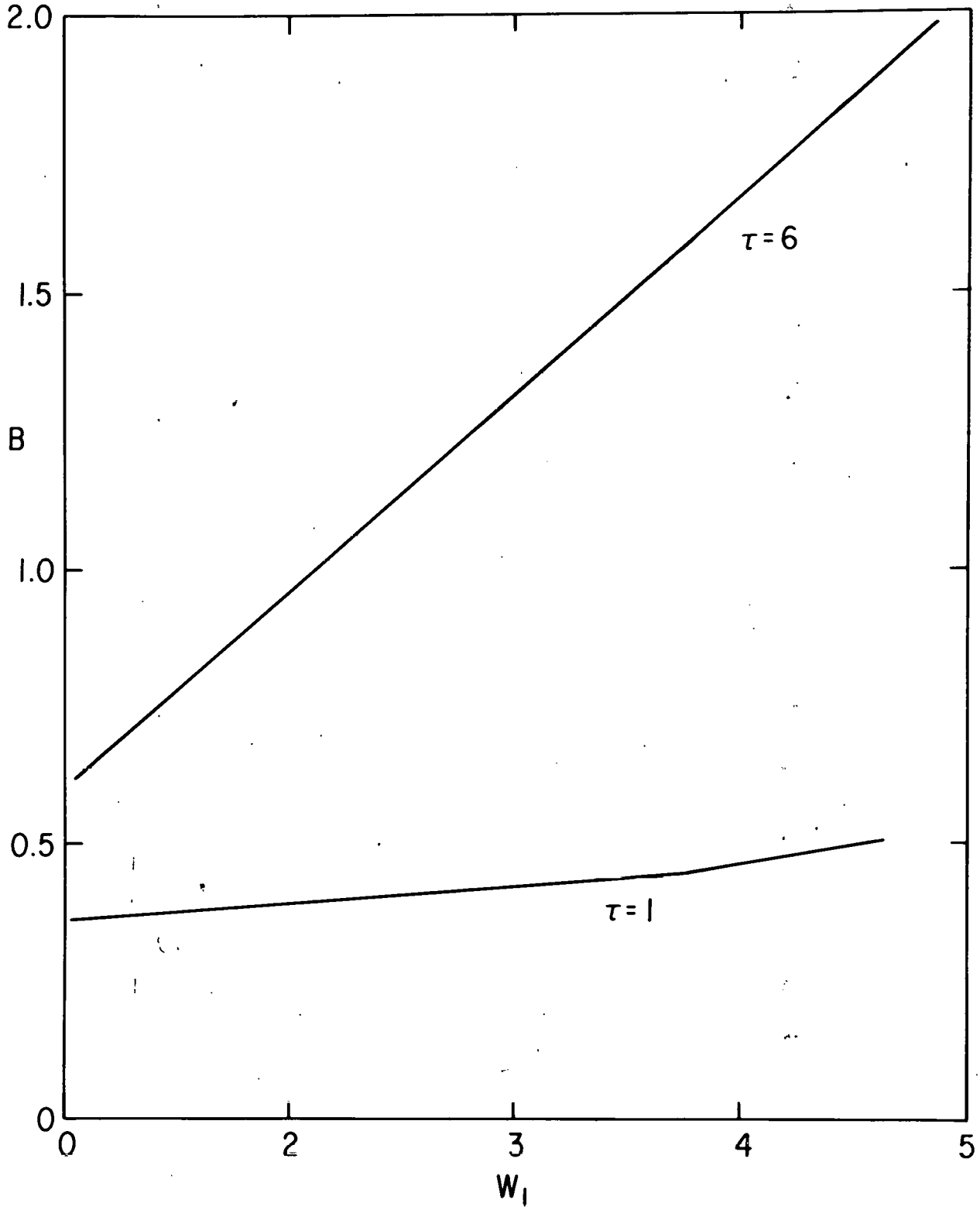

Fig. 6. The maximum value of B as a function of the sideband frequency in units of the lower hybrid frequency, w_1, for electron to ion temperature ratios $\tau = 1$ (the lower curve) and $\tau = 6$ (the upper curve).

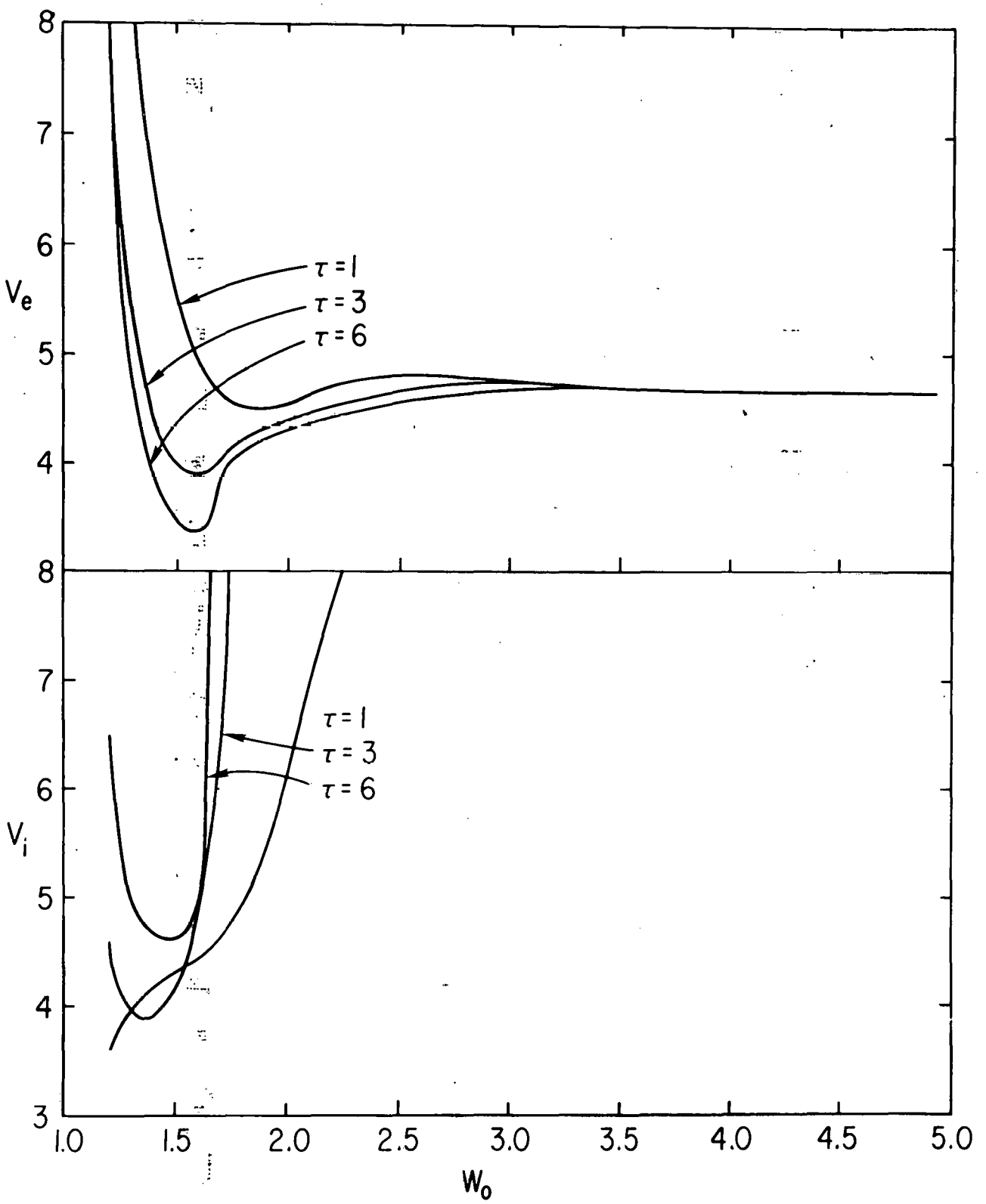

Fig. 7. The values of $V_e = \omega_1/k_{||} v_e$ (upper curves) and $V_i = \omega_1/k_{||} v_i$ (lower curve) as a function of the pump frequency normalized to the lower hybrid frequency for values of electron to ion temperature ratio $\tau = 1,3,6$. Here $v_e(v_i)$ is the electron (ion) thermal velocity.

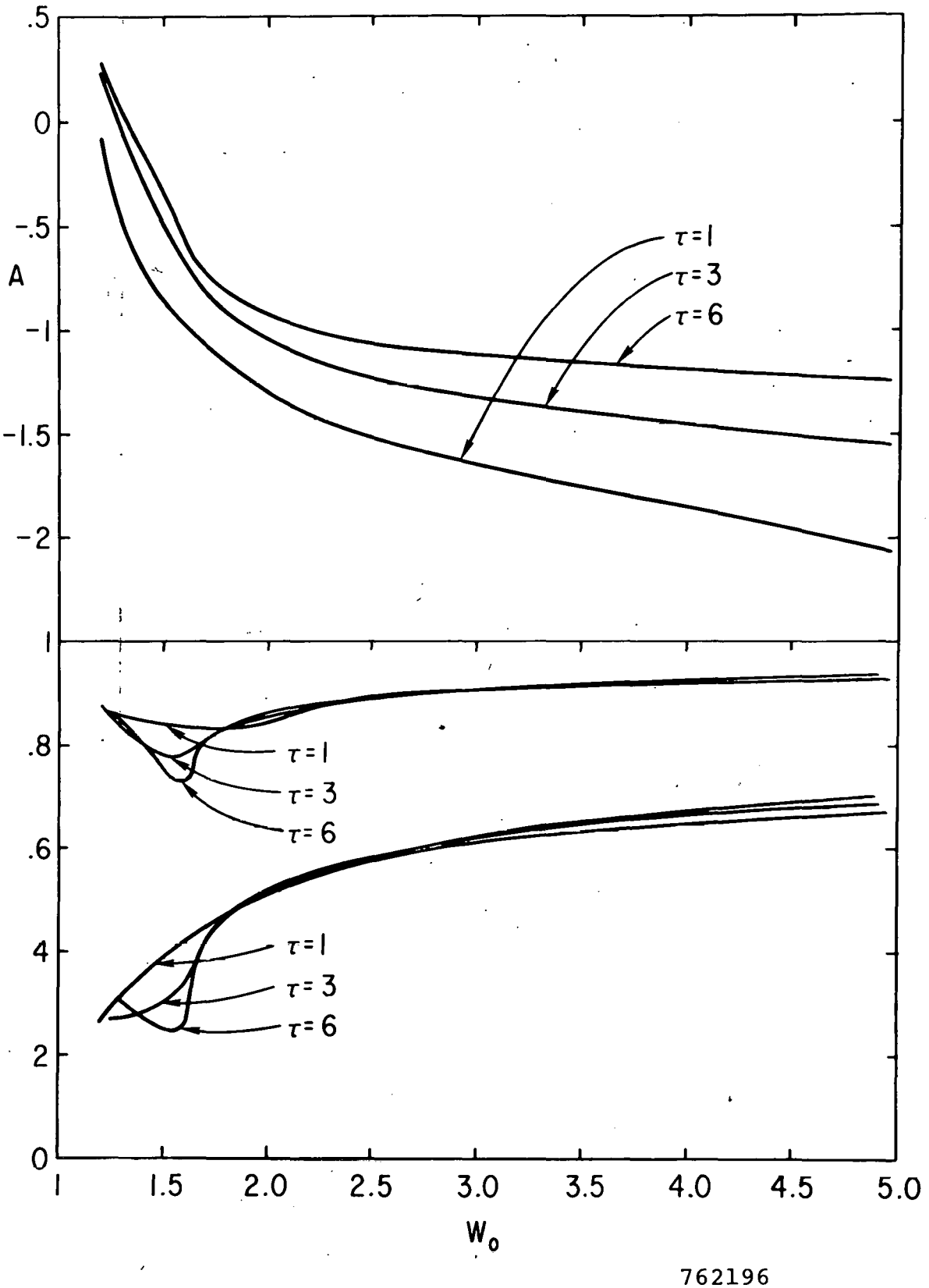

Fig. 8. The logarithm of the amplification factor A given in Eq. (68) maximized with respect to w_1 as a function of w_o for electron to ion temperature ratios $\tau = 1,3,6$ (upper curve). The relative frequency ω_o/ω_1 and $\cos\phi_m$ defined in Eq. (61) that correspond to maximum amplification as a function of w_o for values of $\tau = 1,3,6$.